Molecular Therapy
Methods & Clinical Development
Original Article

Safety and Efficacy of AAV Retrograde Pancreatic Ductal Gene Delivery in Normal and Pancreatic Cancer Mice

Kayla A. Quirin,[1,11] Jason J. Kwon,[1,11] Arafat Alioufi,[1] Tricia Factora,[1] Constance J. Temm,[4] Max Jacobsen,[4] George E. Sandusky,[4] Kim Shontz,[5] Louis G. Chicoine,[5] K. Reed Clark,[6] Joshua T. Mendell,[7,8] Murray Korc,[2,3,9,10] and Janaiah Kota[1,2,3]

[1]Department of Medical and Molecular Genetics, Indiana University School of Medicine (IUSM), Indianapolis, IN 46202, USA; [2]The Melvin and Bren Simon Cancer Center, IUSM, Indianapolis, IN 46202, USA; [3]Pancreatic Cancer Signature Center, Indiana University and Purdue University-Indianapolis (IUPUI), Indianapolis, IN 46202, USA; [4]Department of Pathology, IUSM, Indianapolis, IN 46202, USA; [5]Center for Gene Therapy, Nationwide Children's Hospital, Columbus, OH 43205, USA; [6]Dimension Therapeutics, Cambridge, MA 02139, USA; [7]Department of Molecular Biology, University of Texas Southwestern Medical Center, Dallas, TX 75390, USA; [8]Howard Hughes Medical Institute, University of Texas Southwestern Medical Center, Dallas, TX 75390, USA; [9]Department of Biochemistry and Molecular Biology, IUSM, Indianapolis, IN 43202, USA; [10]Department of Medicine, IUSM, Indianapolis, IN 43202, USA

Recombinant adeno-associated virus (rAAV)-mediated gene delivery shows promise to transduce the pancreas, but safety/efficacy in a neoplastic context is not well established. To identify an ideal AAV serotype, route, and vector dose and assess safety, we have investigated the use of three AAV serotypes (6, 8, and 9) expressing GFP in a self-complementary (sc) AAV vector under an EF1α promoter (scAAV.GFP) following systemic or retrograde pancreatic intraductal delivery. Systemic delivery of scAAV9.GFP transduced the pancreas with high efficiency, but gene expression did not exceed >45% with the highest dose, 5×10^{12} viral genomes (vg). Intraductal delivery of 1×10^{11} vg scAAV6.GFP transduced acini, ductal cells, and islet cells with >50%, ~48%, and >80% efficiency, respectively, and >80% pancreatic transduction was achieved with 5×10^{11} vg. In a $Kras^{G12D}$-driven pancreatic cancer mouse model, intraductal delivery of scAAV6.GFP targeted acini, epithelial, and stromal cells and exhibited persistent gene expression 5 months post-delivery. In normal mice, intraductal delivery induced a transient increase in serum amylase/lipase that resolved within a day of infusion with no sustained pancreatic inflammation or fibrosis. Similarly, in PDAC mice, intraductal delivery did not increase pancreatic intraepithelial neoplasia progression/fibrosis. Our study demonstrates that scAAV6 targets the pancreas/neoplasm efficiently and safely via retrograde pancreatic intraductal delivery.

INTRODUCTION

The pancreas is a primary site of origin for a wide variety of diseases, including diabetes, pancreatic cancer, and pancreatitis.[1] Pancreatic ductal adenocarcinoma (PDAC) has the worst prognosis among pancreatic diseases.[2,3] In the United States, it is the third leading cause of cancer deaths and is projected to become the second leading cause of cancer-related deaths in just over a decade.[4] Although combination chemotherapies such as Nab-paclitaxel/gemcitabine and FOLFIRINOX[5,6] modestly improve survival, the overall 5-year survival rate has not exceeded 8% for the last 30 years.[7] Furthermore, PDAC has a well-characterized mutational profile that plays a key role in disease onset and progression,[8] but the knowledge of these genetic perturbations has yet to yield effective, targeted therapies. A combination of novel gene/cell-based therapeutic strategies with conventional chemo-radiation therapies may improve the survival rate of this deadly cancer.

Pre-clinical animal models, particularly genetically engineered mouse models (GEMMs) of PDAC, have played a pivotal role in understanding the pathobiology of oncogenes/tumor suppressors and in developing new therapeutic strategies.[9–14] Importantly, large-scale deep sequencing data and The Cancer Genome Atlas (TCGA) are identifying new genetic aberrations associated with PDAC pathogenesis.[15–17] Developing pre-clinical mouse models for new oncogenic mutations and/or in combination with well-characterized genetic mutations associated with PDAC progression is a daunting process that typically takes several years. Genome editing tools such as CRISPR/Cas9 in combination with targeted gene delivery could serve as a potential surrogate to transgenic mouse models to study in vivo gene function.[18–21] However, because of its anatomical location, targeted pancreatic gene delivery without safety concerns, particularly pancreatitis, is a major challenge for in vivo gene delivery.

A wide range of non-viral and viral gene delivery systems have been exploited to target the pancreas for therapeutic purposes and functional studies.[22] Non-viral liposomes and nanoparticles have been

Received 8 June 2017; accepted 27 September 2017;
https://doi.org/10.1016/j.omtm.2017.09.006.

[11]These authors contributed equally to this work.

Correspondence: Janaiah Kota, Department of Medical and Molecular Genetics, IUSM, Indianapolis, IN 46202, USA.
E-mail: jkota@iu.edu

commonly employed to deliver conjugated drugs/chemotherapy or therapeutic genes. However, a major limitation with non-viral delivery methods is low efficacy, and they require repeated delivery to achieve therapeutic benefit.[23,24] Viral vectors have been shown to be more efficacious to achieve long-term gene expression with limited off-target effects. Among the viral vectors, integrating lentiviral vectors target the pancreas efficiently (exocrine and endocrine) with no immune response.[25] However, insertional mutagenesis is a major concern and limits its use for in vivo delivery.[26,27] Recombinant adenoviruses (rAds) or adeno-associated viruses (rAAVs) are predominately episomal while still achieving efficient in vivo pancreatic delivery.[28,29] Ad vector-mediated pancreatic gene transfer is transient in nature because of potent host immune responses and vector-mediated cytotoxicity.[30–32] On the other hand, non-integrating AAV vectors are particularly promising in efficiently targeting the whole pancreas,[33–35] have the potential to target specific cell types in the pancreas[36–38] and pancreatic neoplasms,[39] and do not elicit humoral responses or alterations in pancreatic functions.[33–35,39,40] AAV vectors contain a single-stranded DNA (ssDNA) genome with a packaging capacity of ~4.8 kb and are able to mediate long-term transgene expression because of their lack of pathogenicity and low immunogenicity.[41–43] In addition, ssAAV vectors have been engineered to contain a double-stranded DNA (dsDNA) genome (hairpin) to circumvent the requirement for second-strand DNA synthesis, a requisite for transgene expression, and are self-complementary (sc) AAV viral vectors.[44,45] Improved scAAV vectors have been shown to be more efficacious in in vivo gene delivery.[46]

Determining an ideal delivery route with limited off-target effects is another critical component to target the pancreas efficiently. A wide range of gene delivery routes have been exploited, such as direct pancreatic injections,[30,35,47] intraperitoneal delivery,[39,48] systemic delivery,[49,50] in conjunction with clamped hepatic circulation,[33] celiac/hepatic artery delivery,[51] retrograde ductal delivery via pancreaticobiliary ductal infusion,[21,28,34,40] or catheterizing the cystic duct through the gallbladder/common bile duct.[25,33] Among several AAV serotypes tested, AAV8 and AAV9 have been shown to be well-suited for systemic delivery,[52,53] and AAV6 has been shown to transduce the normal pancreas very efficiently via retrograde pancreatic ductal delivery.[33] Accumulating evidence documents the use of AAV to deliver therapeutic molecules/genes to neoplasms, including pancreatic tumors,[39,54] and tissues undergoing rapid degeneration and regeneration.[55,56] However, comprehensive study of the ideal serotype, route, vector dose, and safety profile to target the pancreas with limited off-target effects and in the context of cancer is not well established using scAAV vectors. In this study, we have investigated the use of three scAAV serotypes (AAV6, AAV8, and AAV9) to target the pancreas via systemic delivery or retrograde targeted ductal delivery and optimized the vector dose to maximize pancreatic gene expression. In addition, we evaluated the effect of ductal delivery-mediated pressure on pancreatitis and use of AAV to target the pancreas in a PDAC mouse model driven by $Kras^{G12D}$, a common Kras mutation found in PDAC. We demonstrate that retrograde intraductal delivery of 5×10^{11} scAAV6.GFP viral genomes (vg)/animal transduces the pancreas with >80% transduction efficiency without causing sustained inflammation or fibrosis. Furthermore, we have also shown that scAAV6 transduces acini, epithelial cells, and stromal cells in a PDAC mouse model with persistent long-term gene expression and does not adversely affect PDAC progression.

RESULTS

Comparison of scAAV8 and scAAV9 Serotypes to Target the Pancreas via Systemic Delivery

In both clinical and pre-clinical settings, either direct injection or systemic delivery to the target tissue is a preferred route of administration for therapeutic purposes because of the ease of use. Because direct injection of the pancreas would be more invasive and may not achieve uniform gene expression in the entire pancreas, for our initial studies, we elected systemic delivery. Previously, systemic delivery of ssAAV serotype 8 and 9 (AAV8 and AAV9) has been demonstrated to modestly transduce the pancreas.[52,53] scAAV vectors are known to transduce target tissues with higher efficiency compared with ssAAV vectors.[46] To test the ideal serotype for systemic delivery, an scAAV viral vector expressing GFP under an EF1α promoter (scAAV.GFP) (Figure 1A) was packaged using AAV8 and AAV9 serotypes, 1×10^{12} vg/animal were delivered systemically (n = 3 mice/group) to normal C57BL/6 mice, and animals were sacrificed 3 weeks post-vector administration. As documented by fluorescence microscopy for GFP expression, AAV9 showed a modestly higher pancreatic transduction efficiency (14.6% ± 2.5% SEM) compared with AAV8 (11.5% ± 0.2% SEM) (Figure 1B) with some off-targets (Figures S1A and S1B).

To test the ideal dose for achieving maximum pancreatic transduction efficiency via systemic delivery of scAAV9.GFP, we compared three different doses ranging from 1×10^{12}–5×10^{12} vg/animal. Although an increase in vector dose improved the transduction percentages, none of the tested doses reached >45% pancreatic transduction efficiency (Figures 1C and 1D). This level of gene expression may be sufficient to develop therapeutic strategies for non-neoplastic tissues, but in the context of cancer, optimal transduction efficiency is preferred for therapeutic benefit and functional studies. A further dose increase via systemic delivery may improve the transduction efficiency, but producing large quantities of clinical vectors for systemic dosing of adult PDAC patients without causing toxicity with high dose may be challenging.

Retrograde Intraductal Infusion of scAAV6 Transduces the Pancreas Uniformly and Efficiently

A wide range of gene delivery methods was previously evaluated to directly target the pancreas, such as retrograde pancreatic ductal delivery by direct injection of the distal common bile duct,[21,34] cannulation of the common bile duct through the gallbladder/cystic duct, and intravenous injection coupled with liver blockage.[33] Although each of these methods was shown to be effective to transduce the whole pancreas or various cell types of the pancreas (acini, islets of Langerhans, and ductal cells), we elected for retrograde ductal

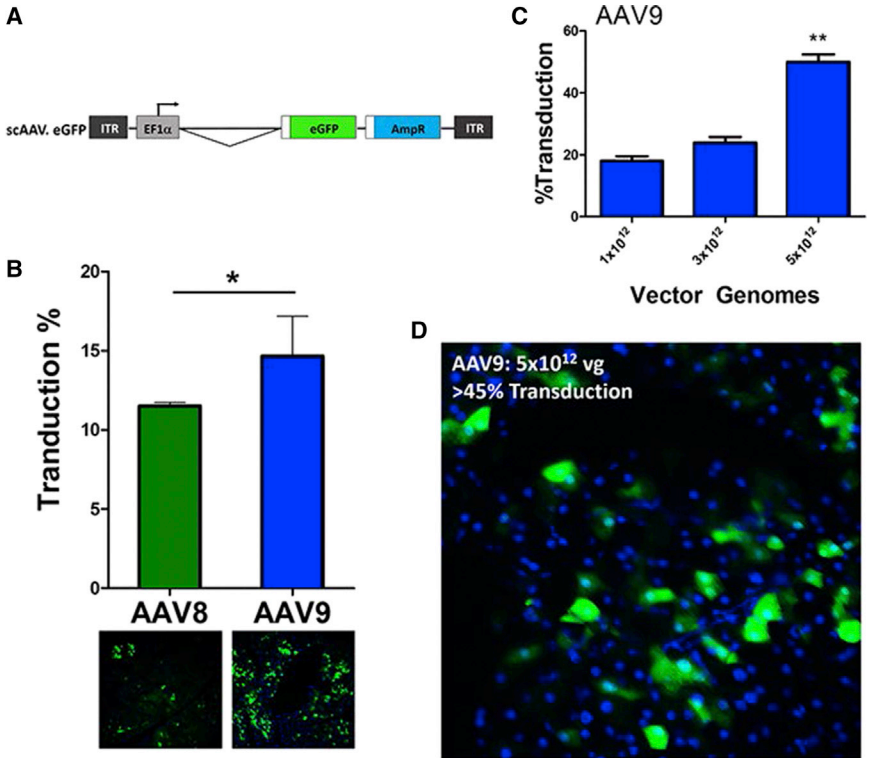

Figure 1. Comparison of scAAV8 and AAV9 to Target the Pancreas via Systemic Delivery

(A) Schematic of the scAAV.GFP vector. (B) Quantification of GFP expression in C57BL/6 mice administered 1×10^{12} vg/animal of scAAV8.GFP and scAAV9.GFP via tail vein injection (n = 3/group), as determined by percentage GFP^+ acinar cells. A representative image of global pancreatic GFP expression is shown below each graph column; ~6-μm frozen tissue sections. (C) Quantification of GFP expression in C57BL/6 mice administered scAAV9.GFP at various doses via tail vein injection (n = 3/group), as determined by percentage GFP^+ acinar cells. (D) Representative global pancreatic GFP expression of C57BL/6 mice dosed with 5×10^{12} vg scAAV9.GFP 3 weeks post-vector administration. 20× magnification. Data represent mean ± SEM; $^*p < 0.05$.

delivery via cannulation of the common bile duct to evaluate its safety profile and use in cancer settings using scAAV vectors.

Initially, to optimize the conditions for cannulation and retrograde ductal delivery, we dosed a cohort of mice with Evans Blue dye. As elaborated in Materials and Methods, a customized 10-mm catheter was advanced through the gallbladder and cystic duct to the common bile duct (Figure 2A). A microclamp was placed on the bile duct and sphincter of Oddi to prevent vector leakage into the liver and small intestine, and 100 μL of Evans Blue was injected over 2–3 min to target the pancreas. We observed a uniform distribution of Evans Blue in the entire pancreas (Figure 2A).

Subsequently, to test the efficacy of rAAV to target the pancreas, in our initial studies, we packaged scAAV.GFP with the AAV6 serotype, which has been shown to efficiently target the pancreas.[33,34] We administered 1×10^{11} vg/animal of scAAV6.GFP via retrograde ductal delivery, and animals were sacrificed 3 weeks later for global pancreatic GFP expression analysis. As documented under direct fluorescence, scAAV6 transduced the pancreas with uniform GFP expression (Figure 2B).

Identification of an AAV Serotype to Efficiently Target the Pancreas via Retrograde Intraductal Infusion

Single-stranded AAV 6, 8, and 9 serotype vectors have been shown to transduce the pancreas efficiently via retrograde pancreatic intraductal delivery.[57] However, the efficiency of scAAV vectors has not yet been determined. To address this question, we compared scAAV.GFP serotypes 6, 8, and 9, and dosed a cohort of C57BL/6 mice for each serotype (n = 3–4 mice/group) with 1×10^{11} vg/animal via retrograde pancreatic ductal delivery. 3 weeks post-vector infusion, animals were sacrificed, and pancreata were collected from each animal to compare GFP transduction efficiency. As documented by fluorescent microscopy, scAAV6 and scAAV9 transduced acinar cells (exocrine cells) more efficiently with 53% ± 3.8% SEM and 52% ± 2.7% SEM, respectively (Figure 2C), compared with scAAV8 (21.7% ± 5.9% SEM). Similarly, scAAV6 transduced ductal cells (48.2% ± 10.25% SEM) more efficiently compared with scAAV8 (12.1% ± 3.2% SEM) and scAAV9 (13.6% ± 3.7% SEM) (Figure 2D). Furthermore, scAAV6 transduced pancreatic islet cells with relatively higher efficiency (82.1% ± 3.1% SEM) compared with scAAV8 (16.3% ± 3.1% SEM) and scAAV9 (30.5% ± 5.0% SEM) (Figure 2E). To achieve maximum pancreatic transduction via intraductal delivery, we dosed a cohort of mice (n = 3–5 mice/group) with three escalating doses (1×10^{11}, 3×10^{11}, and 5×10^{11} vg/animal) using scAAV6.GFP. Quantification of the transduced exocrine acinar cells showed an increase in transduction percentages, with maximum gene expression achieved at 5×10^{11} vg (Figure 2F).

Because scAAV6 and scAAV9 showed comparable transduction efficiency at the lowest dose (1×10^{11} vg/animal), to achieve maximum pancreatic gene expression in this model, we compared the transduction efficiency of AAV6 and AAV9 at a dose of 5×10^{11} vg/animal. AAV6 had statistically significant higher pancreatic GFP expression (86% ± 2.4% SEM) compared with AAV9 (75% ± 1% SEM) (Figures 3A and 3B). We also examined GFP expression in the livers of these mice (a common off-target of intraductally dosed mice),[40,57] and AAV9 had relatively higher liver transduction percentages compared with AAV6 (Figure 3A). To further confirm this observation, we quantified transduced vector genomes of the pancreas and liver by

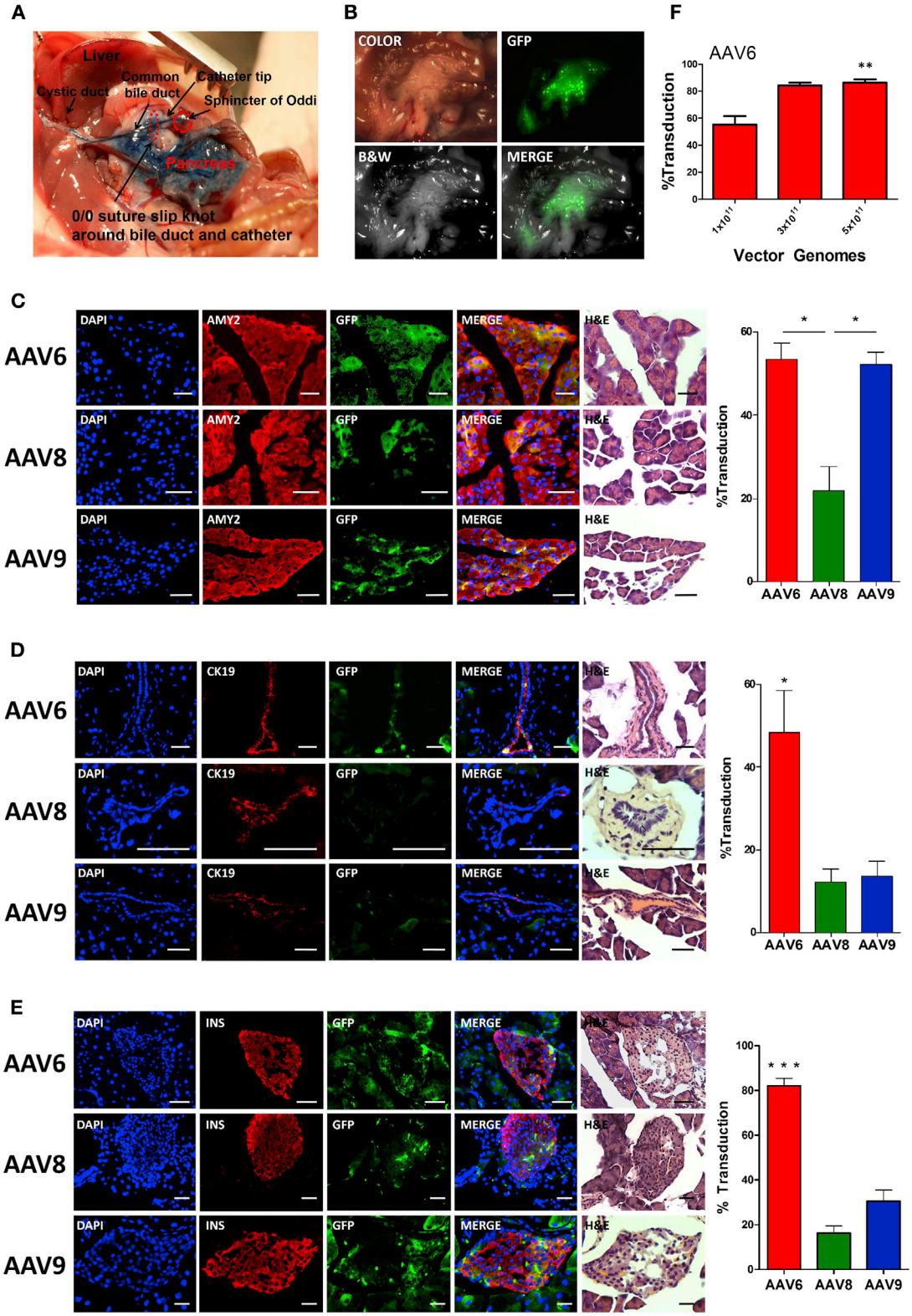

(legend on next page)

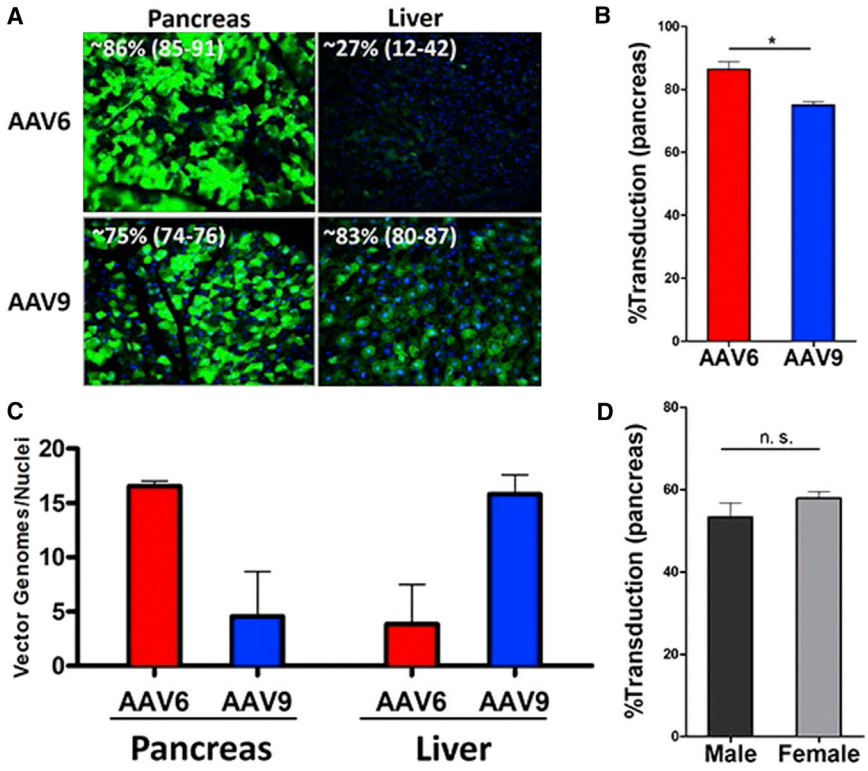

Figure 3. scAAV6 Has Increased Specificity in Transducing the Pancreas Compared with scAAV9

C57BL/6 mice were dosed with scAAV6.GFP or scAAV9.GFP at 5×10^{11} vg/animal. (A) Pancreatic and liver GFP^+ expression was determined via fluorescence microscopy. Representative pancreatic and liver images are shown for each serotype at 20× magnification. (B) Quantification of pancreatic and liver transduction was determined by the percentage of GFP^+ acinar cells and hepatocytes, respectively. (C) DNA was isolated from pancreata and livers of scAAV6.GFP or scAAV9.GFP retrograde intraductally infused C57BL/6 mice and subjected to qPCR analysis for AAV genome copy numbers. Data represent mean ± SEM. *$p < 0.05$. (D) Quantification of pancreatic GFP expression was determined in male and female C57BL/6 mice dosed with 5×10^{11} vg of scAAV6.GFP.

qPCR. AAV6 had more specificity in targeting the pancreas with more vector genomes compared to AAV9, whereas AAV9 had relatively very high vector genome copies in the liver compared with AAV6 (Figure 3C). We further tested this phenomenon in animals dosed with 5×10^{11} vg/animal of AAV6 and AAV9 and found that AAV6 has more specificity in transducing the pancreas compared with AAV9 (Table S1). scAAV6-mediated GFP expression was not found in any other tissues in the body, including the heart, lung, and kidney (Figure S1C). Finally, to test the effect of murine gender on AAV6-mediated pancreatic transduction, we dosed a cohort of C57BL/6 males and females with 5×10^{11} vg of scAAV6.GFP (n = 3 mice/group) and found that gender did not have a significant effect on pancreatic transduction (Figure 3D).

AAV6 Targets and Shows Long-Term Gene Expression in Acinar, Epithelial, and Stromal Cells in PDAC Mice

To test the feasibility of using scAAV6 to target the pancreas of PDAC mice, we dosed a cohort of a well-characterized PDAC mouse model, *LSL-Kras^{G12D}*; *Pdx1-Cre* (KC) with scAAV6.GFP at 1 month of age via intraductal delivery. As documented via fluorescence microscopy and immunohistochemistry for GFP, scAAV6 transduced KC mice pancreata efficiently 3 weeks post-vector administration (Figure S2). To test AAV-mediated long-term gene expression, we collected the pancreata of scAAV6.GFP intraductally dosed KC mice 5 months post-infusion and found persistent GFP expression (Figure 4; Table 1) in acinar, epithelial/cancer, islet, and pancreatic stellate cells (PSCs). scAAV6 transduced PSCs (28.5% ± 4.7 SEM) and pancreatic intraepithelial neoplasm (PanIN)/ducts (7.6% ± 2.6% SEM) with relatively lower efficiency compared with acinar cells (55.0% ± 16.5% SEM) and islets cells (41.5% ± 5.5% SEM) (Figure 4; Table 1). The efficiency of scAAV6 to target neoplastic tissues needs to be further optimized through understanding the mechanisms associated with AAV6 transduction in the various pancreatic compartments. Nevertheless, our findings provide evidence that persistent gene expression can be achieved in proliferating epithelial and stromal cells in the context of a genetically engineered mouse model of pancreatic cancer.

Retrograde Intraductal Delivery Is Safe, with No Evidence of Pancreatitis in Normal Pancreata, and Does Not Enhance Disease Progression in PDAC Mice

An increase in pancreatic intraductal pressure is known to cause inflammation/pancreatitis, a known risk factor for PDAC.[58–60] To evaluate the effect of intraductal delivery-mediated pressure on

Figure 2. Optimization of Retrograde Intraductal Infusion via Catheterizing the Common Bile Duct through the Gallbladder and Cystic Duct

(A) Uniform Evans Blue dye delivery to the entire pancreas via the retrograde intraductal infusion procedure. (B) A C57BL/6 mouse was dosed with 1×10^{11} vg of scAAV6.GFP via retrograde intraductal infusion, and pancreatic GFP expression was observed via direct fluorescence. (C–E) A cohort of C57BL/6 mice was dosed with scAAV6.GFP, 8, or 9 at 1×10^{11} vg/animal (n = 3–4/group). Serial sections of frozen (6 μm) pancreatic tissue collected 3 weeks post-vector infusion were stained for (C) amylase (AMY2, acinar cells), (D) Cytokeratin 19 (CK19, ductal cells), or (E) insulin (INS, islets) or with H&E to quantify cell-specific GFP transduction percentages. GFP, green; AMY2, CK19, or INS, red; DAPI, blue; 20× magnification; scale bar, 50 μm; representative images are presented. (F) A cohort of C57BL/6 mice was intraductally infused with different doses of scAAV6.GFP (n = 4–6/group), and the percentage of GFP^+ acinar cells was determined. Data represent mean ± SEM, *$p < 0.05$, **$p < 0.01$, ***$p < 0.001$.

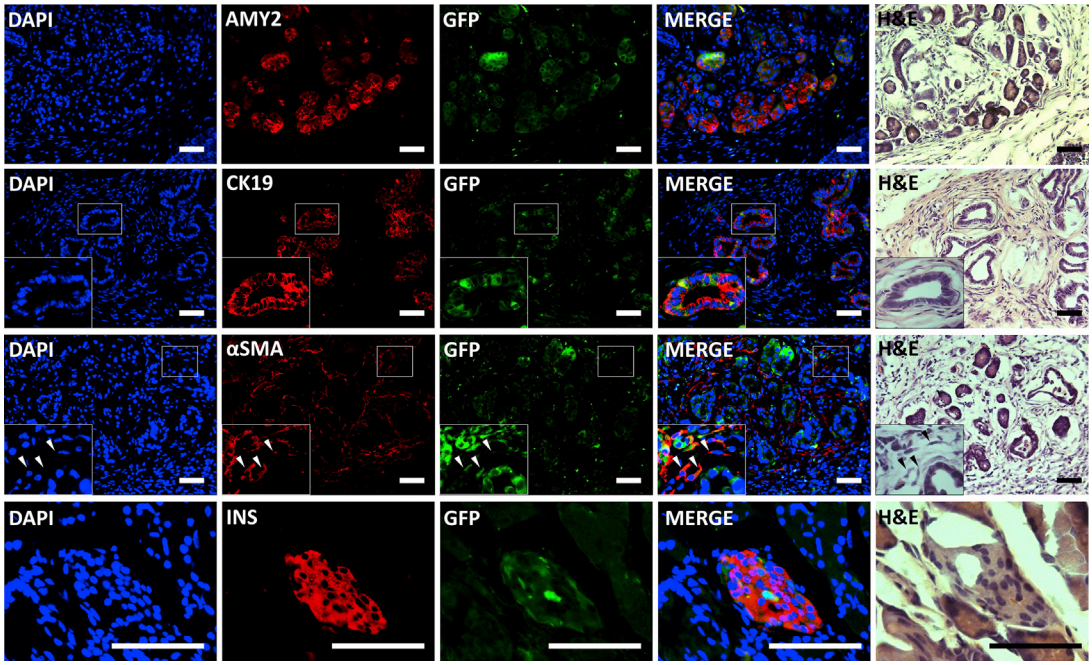

Figure 4. Retrograde Pancreatic Intraductal Delivery of scAAV6 Targets Acinar, Epithelial, and Stromal Cells and Shows Long-Term Gene Expression in PDAC Mice

5×10^{11}vg of scAAV6.GFP was dosed in 1-month-old KC mice, and pancreata were collected 5 months post-delivery for the late time point and stained for amylase (AMY2), CK19, αSMA, or insulin (INS) to identify acinar cells, ductal cells, PSCs, and islet cells, respectively. Serial sections were stained with H&E, and representative images are presented. GFP, green; AMY2, CK19, αSMA, or INS, red; DAPI, blue; 20× magnification; scale bars, 50 μm; inset, 40×; arrows indicate $\alpha SMA^+/GFP^+$ PSCs.

pancreatic inflammation, we dosed a cohort of C57BL/6 mice with PBS and monitored serum pancreatitis markers, amylase and lipase.[61–63] We observed a rapid increase in amylase and lipase levels 3 hr post-vector delivery that resolved within a day of intraductal infusion (Figures 5A and 5B). By histopathological examination, there was minimal to no pancreatic inflammation seen at various time points (Figure 5C), except for a detectable peri-pancreatic fat lymphoid response in a few mice at 2–5 days post-infusion (Figure 5D). We also stained pancreata with a B cell marker (B220) to monitor lymphoid responses. Normal mice were negative for B220 at all time points, 1–15 days post-infusion (Figure 5C; Table S2). In addition, to evaluate the effect of intraductally mediated pressure on pancreatic fibrosis, we stained pancreata of C57BL/6 mice with trichrome (Figure 5C) and found no significant increase in pancreatic fibrosis in intraductally dosed mice compared with non-injected control mice (Figure 5E).

Finally, to evaluate the effect of intraductal delivery-mediated inflammation on PDAC progression, we performed histopathological analysis in KC mice dosed with PBS or scAAV6.GFP at 5 months post-infusion. As shown in Figures 6A–6C, there was no significant difference in the size and number of PanIN grades between intraductally infused KC mice and controls. Furthermore, intraductally infused KC mice were negative for B220 staining <1% (Table S3), and there was no significant increase in pancreatic fibrosis based on trichrome staining (Figure 6D).

DISCUSSION

Previously, numerous non-virally and virally mediated delivery methods were employed to deliver therapeutic molecules/genes to the pancreas via direct,[30,35] systemic,[50,51] intraperitoneal,[39] and retrograde ductal delivery.[21,25,33] Among the various vector systems and routes of administration, retrograde ductal delivery of AAV demonstrated efficient pancreatic gene expression.[33,34,40] However, the safety and efficacy of retrograde ductal delivery regarding development of pancreatitis, a known risk factor for PDAC, and use of AAV in cancer settings have not been well established. Here we compared the use of different AAV serotypes for efficient delivery to the pancreas via intravenous (AAV8 and AAV9) or retrograde pancreatic ductal delivery (AAV6, AAV8, and AAV9) using double-stranded scAAV vectors expressing GFP under a ubiquitous promoter, EF1α. Our results indicate that retrograde pancreatic ductal delivery of scAAV6 via catheterizing the common bile duct through the gallbladder/cystic duct transduces various cell types of the pancreas, such as acini, ducts, and islets, efficiently compared with scAAV8 and scAAV9 without inducing pancreatitis. Furthermore, as a proof of concept, we showed that retrograde pancreatic ductal delivery of scAAV6 transduces acini, epithelial cells, and stromal cells in a pre-clinical PDAC mouse model and demonstrated persistent gene expression up to 5 months post-infusion.

Although direct pancreatic targeted delivery is very robust and achieves maximum gene expression because of the retroperitoneal

Table 1. Percent Transduction in Various Pancreatic Compartments of KC Mice

Pancreatic Compartment	% Transduction
Acini (AMY2)	55.0% ± 17% SEM
Epithelial cells (CK19)	7.6% ± 2.6% SEM
PSCs (αSMA)	28.5% ± 4.7% SEM
Islets (INS)	41.5% ± 5.5% SEM

location of the pancreas, less invasive systemic gene delivery is a preferred method of choice in clinical settings. In an attempt to identify a serotype that can be used to efficiently target the pancreas via systemic delivery, we compared the pancreatic transduction efficiency of scAAV8 and scAAV9. scAAV9 showed a relatively higher pancreatic transduction efficiency compared with scAAV8 via systemic gene delivery. However, maximum acinar gene expression was <60% in spite of the high scAAV9 dose, 5×10^{12} vg/animal. Previous reports indicate that systemic delivery of ssAAV9 transduces the pancreas robustly at a relatively low vector dose (1.8×10^{12} vg/animal).[53] Perhaps the lower transduction percentage observed in gene expression could be due to the use of an endogenous promoter, EF1α, compared with the CMV promoter used in previous studies.[53] We used scAAV9 instead of ssAAV9, which is known to transduce more efficiently compared with ssAAV.[46] In spite of utilizing scAAV vectors, pancreatic transduction efficiency via systemic delivery was significantly lower compared with previous reports that used ssAAV vectors. The low pancreatic transduction percentage via systemic delivery may fulfill the required gene expression levels for studies involving pancreatic origin diseases such as diabetes, where restoration of a few functional copies of a gene may have a functional/therapeutic effect.

Similar to previous reports using ssAAV,[33,34,40] our observations demonstrate that efficient pancreatic transduction can be achieved via retrograde pancreatic ductal delivery of scAAV, a surgical procedure that parallels clinical endoscopic retrograde cholangiopancreatography (ERCP) in humans. Among the three AAV serotypes tested via pancreatic ductal delivery, AAV6 transduced the whole pancreas and various pancreatic compartments (acini, ducts, and islets) more efficiently compared with AAV8 and AAV9. The transduction efficiency of intraductally mediated delivery of AAV6 via the EF1α promoter in various pancreatic compartments is comparable with previous reports using a CMV promoter.[34] In addition, AAV6 has relatively minimal liver transduction, a common off-target of intraductally dosed mice.[33,40] AAV9 had comparable pancreatic targeting efficiency to AAV6 but showed higher liver transduction. The increase in liver transduction with AAV9 may be due to the higher abundance of receptors and/or co-receptors for AAV9 in hepatocytes and is consistent with a previous report indicating that AAV9 transduces the liver more efficiently upon systemic injection compared with AAV6.[53] Because the liver is a common site for metastasis in pancreatic cancer, AAV9 may be more appealing for gene delivery at later disease stages in a metastatic context.

Our results also demonstrate that retrograde pancreatic ductal delivery is safe and does not induce sustained pancreatitis in mice. Although we observed a transient increase in pancreatitis markers ~1 day post-infusion, amylase and lipase levels resolved within 24 hr. Furthermore, no significant increase in lymphoid proliferation or fibrosis was observed by histopathological examination in intraductally infused mice. Pancreatitis is a known risk factor for PDAC, and patients with chronic or acute pancreatitis have a higher risk of developing cancer and can experience enhanced cancer progression. To test the safety of intraductally mediated delivery in cancer settings, we evaluated PanIN progression in a well characterized PDAC mouse model dosed with PBS and scAAV6.GFP and found no effect on cancer progression.

Finally, to test the potential use of scAAV to target pancreatic neoplasm via retrograde delivery, we dosed 1-month-old KC mice, a $Kras^{G12D}$-driven PDAC mouse model, with scAAV6.GFP and found efficient transduction in acinar and ductal cells (the primary cells of origin for PDAC) and PSCs, the major cells responsible for PDAC stromal accumulation.[64,65] Furthermore, we observed long-term GFP expression in $amylase^+$ acini, $CK19^+$ ductal cells, and αSMA^+ stromal cells at 6 months of age, a time point when KC mice develop more advanced PanIN 2–3 lesions.[12] In addition to our work, a recent report demonstrated the use of capsid-optimized scAAV8 to target pancreatic neoplasms via intraperitoneal administration.[39] Although capsid-optimized AAV8 has limited off-target effects compared with WT AAV8, there was a robust gene expression in the liver comparable with the pancreas, which could be improved in combination with the retrograde pancreatic targeted delivery we employed here to efficiently target the pancreas.

Our current work and recent reports from others[39] indicate the potential applicability of AAVs to deliver therapeutic molecules/genes to various compartments of PDAC and affect tumor progression. Similarly, previous reports indicate that ductal delivery of AAVs in combination with cell-specific promoters serves as an excellent surrogate for pancreatic cell lineage studies.[36–38] Another potential application of this work is using AAVs as a non-integrating delivery vehicle for genome editing-mediated functional studies. The latest developments in genome sequencing technologies are rapidly unravelling new genes underlying various human diseases.[66] However, alternative and more rapid methods than transgenic mouse models are required for in vivo characterization of new genes to quickly translate basic research findings into the clinic.[20]

Genome editing tools such as CRISPR/Cas9 have become useful to study gene function.[67–69] In fact, surrogate use of retrograde pancreatic targeted delivery of Cre-recombinase or CRISPR/Cas9 via adeno- and lentiviral vectors has been elegantly demonstrated for the development of PDAC mouse models.[21] The AAV-mediated pancreatic targeted delivery described here in combination with cell-specific promoters is amenable to genome editing technologies to study in vivo gene function and will aid in accelerating basic

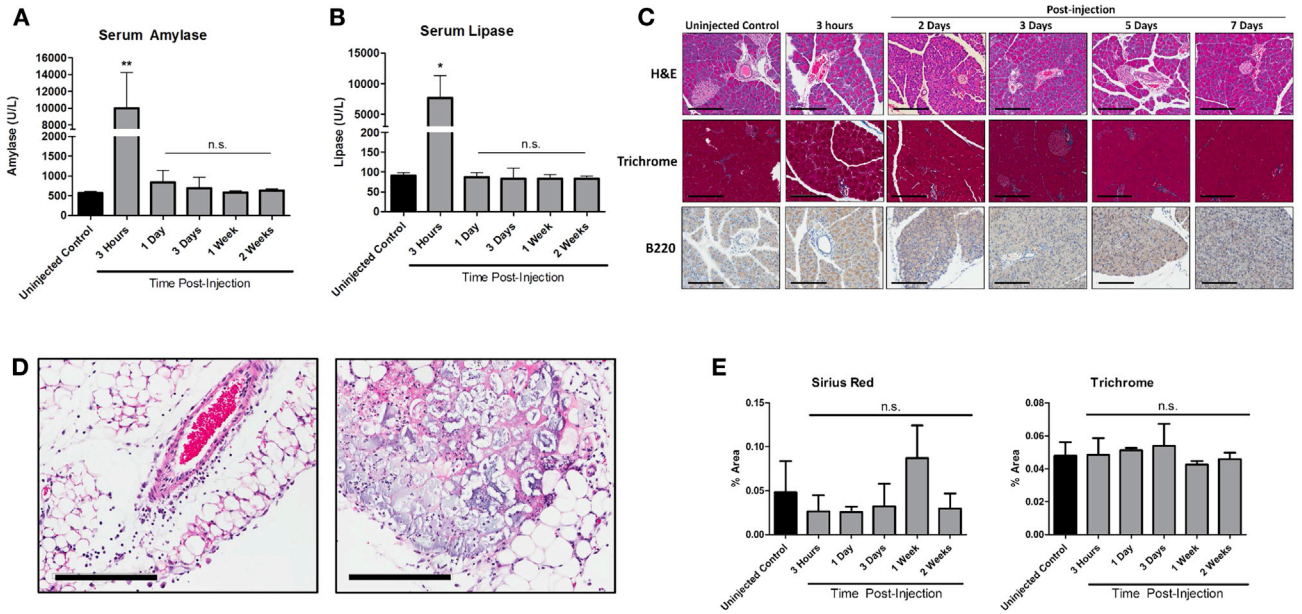

Figure 5. Retrograde Pancreatic Intraductal Delivery Is Safe and Does Not Induce Chronic Pancreatitis

(A and B) Serum samples collected from intraductally dosed (100 μL PBS) C57BL/6 mice were analyzed for (A) amylase and (B) lipase. Data represent mean ± SEM; *$p < 0.05$; **$p < 0.01$; n.s., non-significant. (C) Representative H&E, trichrome, and B220 images; 20× magnification; scale bars, 200 μm. (D) Representative fat lymphoid responses observed at early time points (1–3 days, H&E). Scale bars, 200 μm, 20× magnification. (E) Mean Sirius Red- or trichrome-positive area (percent) of pancreatic tissue in retrograde pancreatic intraductally injected C57BL/6 (1–14 days post-infusion) mice (n = 3–4 mice/time point). Data represent mean ± SEM.

research findings into the clinic. The AAV platform is more attractive because its safety profile and ideal serotypes are well established to target various tissues. Although viral vectors may not replace mouse models, they will serve as great tools to further advance pre-clinical research by studying gene function alone or in combination with known genetic causes. Retrograde ductal delivery will be a useful tool in studying the gene function of non-coding RNAs, such as microRNAs (miRNAs). Often a single miRNA has several family members[70–72] that are expressed in a tissue- and cell-specific manner. Developing a tissue/cell-specific mouse model for individual miRNA family members in combination with underlying disease-related genetic mutations is a daunting process. Using a similar method as described here, miRNA families can be inhibited by developing AAV vectors for miRNA inhibition strategies such as tough decoys (TuDs), anatagomirs, etc. Proof-of-concept studies suggest the use of viral vectors to inhibit endogenous miRNAs.[73–75] Similarly, delivering synthetic miRNA duplexes for therapeutic purposes has potential limitations associated with half-life and requires repeated administration.[76] Evidence suggests that the use of AAVs for in vivo delivery of therapeutic miRNA has no associated toxicity.[77,78]

In summary, our study demonstrates that scAAV6 targets both normal and neoplastic pancreata via retrograde ductal delivery. Our previous work and that of others support the use of AAV vectors to target a wide variety of neoplasms[54,78–83] and target tissues undergoing multiple cycles of degeneration-regeneration.[84–86] However, a number of pre-clinical studies need to be performed before this method reaches clinical settings because of the fact that AAVs are non-integrating vectors, and their expression is lost in rapidly proliferating neoplastic tissue. First, the transduction efficacy in KC mice needs to be evaluated in animals dosed at early stages of PanIN-1A/B development at <2 months of age versus more advanced stages of PanIN-2/3 lesions at ~9 months of age.[12] Second, transduction efficiency and long-term gene expression need to be evaluated in a more aggressive PDAC mouse model that recapitulates the aggressive form of human disease, such as $Kras^{G12D}$; $p53^{R172H}$; *Pdx1-Cre* (KPC), etc.[11] Third, further refinements to the gene transfer vector will be necessary to allow for cell-specific targeting of pancreatic tumors, similar to previous reports.[36–38] Fourth, the underlying mechanisms for efficient scAAV6 pancreatic transduction in neoplastic tissues and AAV receptor profiling in various pancreatic compartments and cancer cells need to be evaluated, particularly to further optimize the transduction efficiency of neoplastic tissue. Fifth, the present study also points out the limitations of AAVs to achieve high levels of long-term gene expression in rapidly dividing neoplastic tissue. Nevertheless, our results point out the potential use of AAVs in early stages of cancer development, when transient therapeutic gene expression may have an effect on disease progression and could be used to treat patients with pancreatitis, PDAC patients prophylactically, or as an adjunct therapy. Furthermore, targeted AAV-mediated in vivo gene delivery to various pancreatic compartments will serve as a great tool in pre-clinical functional studies.

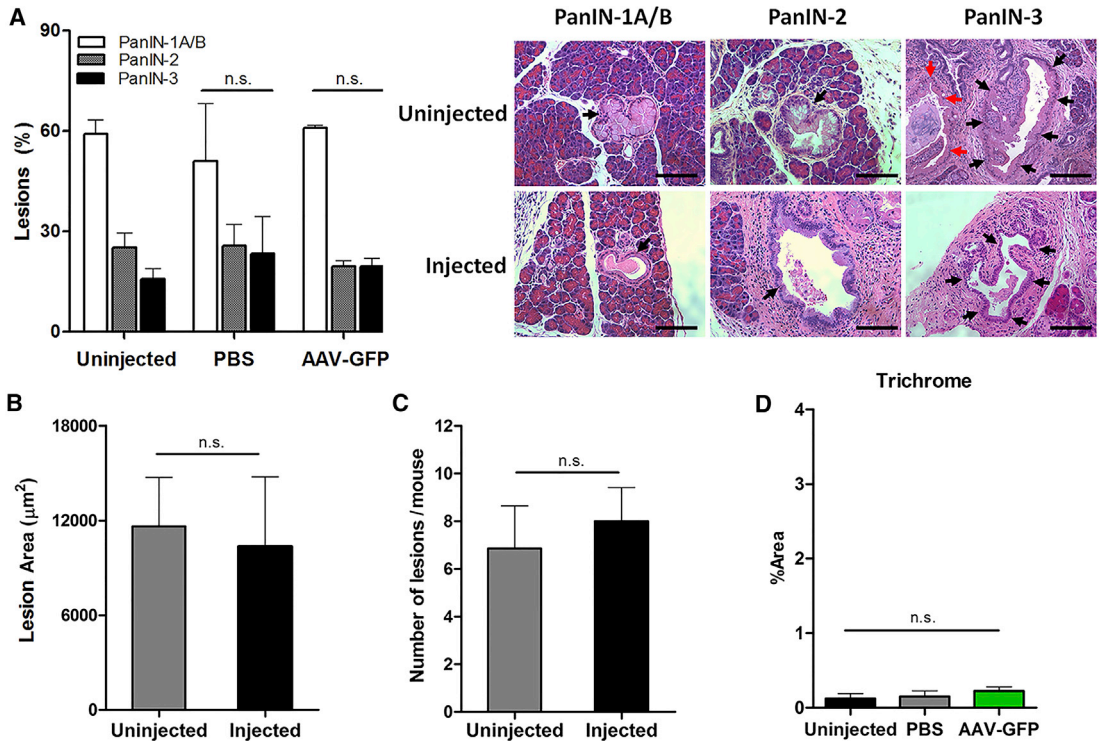

Figure 6. Retrograde Pancreatic Intraductal Delivery Has No Effect on PDAC Progression in KC Mice

(A) Pancreata collected from KC mice 5 months post-infusion (100 μL of PBS or 5×10^{11} vg scAAV6.GFP) were analyzed and compared against un-injected control mice for (A) PanIN grades (1A/B, 2, and 3) (n = 3–5 mice/group), and representative images for each PanIN grade, indicated by black arrows. An adjacent PanIN-3 lesion is indicated by red arrows. 20× magnification; scale bar, 100 μm. (B and C) Average area of PanIN lesions (B) and number of PanIN lesions per mouse (C) (n = 5–7 mice/group). (D) The trichrome staining-positive percentage area was quantified (n = 3–5 mice/group). Data represent mean ± SEM. The p values were determined by t test.

MATERIALS AND METHODS

AAV Vector Production

A self-complementary recombinant AAV vector encoding a GFP under an ubiquitous EF1α promoter has been described previously.[78] Recombinant AAV vectors were produced by a standard triple transfection calcium phosphate precipitation method using HEK293 cells (ATCC, CRL-1573). The production plasmids were scAAV.GFP, rep2-cap6/8/9 modified AAV helper plasmid encoding cap serotype 6, 8, or 9, and an adenovirus type 5 helper plasmid (pAdhelper) expressing adenovirus E2A, E4, ORF6, and VA I/II RNA genes. Purification was accomplished from clarified HEK293 cell lysates by sequential iodixanol gradient purification and ion exchange column chromatography using a linear NaCl salt gradient for particle elution. vg titers were determined by qPCR using EF1α primer and probe set as described previously.[78,87]

AAV Transduction Efficiency

Fresh tissues were harvested and fixed in 4% paraformaldehyde, followed by overnight incubation in 30% sucrose, and then embedded in OCT. Tissue blocks were cut into 6-μm sections using a Leica cryostat. Transduction efficiency was determined by counting the number of GFP^+ and negative acinar cells, ductal cells, PSCs, or islets using four random 20× GFP and DAPI overlay images. GFP transgene qPCR was performed on total DNA isolated from pancreatic and liver tissues. Total tissue DNA was isolated using the Gentra Puregene kit (QIAGEN) according to the manufacturer's instructions. 60 ng of DNA (10,000 cell equivalents) was used as a PCR template in triplicate reactions, and vg numbers were extrapolated from a linearized plasmid standard. Vector genome/cell calculations assumed 6 pg of total DNA per cell using GFP primer and probe set as described previously.[78]

Histology and Microscopy

Whole-Organ Pancreatic GFP Expression

At necropsy, the abdominal cavity was opened, and the whole pancreas was imaged for GFP expression using a Leica dissection fluorescence microscope.

H&E and Masson's Trichrome/Sirius Red Staining

After formalin fixation, specimens were dehydrated through a graded series of ethanols, cleared in two changes of xylenes, and infiltrated through 3 changes of melted paraffin. The specimens were then embedded in melted paraffin and allowed to harden. Thin sections (~5 μm) were cut using a rotary microtome equipped with disposable steel knives. Sections were flattened in a heated water bath, floated onto microscope slides, and dried. Serial sections were de-paraffinized

and stained with H&E, Masson's trichrome stain (Sigma-Aldrich, HT15-1KT), and Picro-Sirius Red to detect pancreatic fibrosis following standard histological procedures or according to the manufacturer's instructions. Similarly, serial frozen sections (~5–7 μm) were stained with H&E.

B220 Immunohistochemistry

Antigen retrieval was performed at high pH in the Dako Link Pretreatment module. After treating with a protein block (Dako) for 10 min, slides were incubated with CD45 primary antibody (clone B220, BD-550286, 1:50) for 60 min, followed by biotinylated anti-rat immunoglobulin G (IgG) (Jackson ImmunoResearch) for 30 min, and finally with LSAB2-SA-HRP (Dako) for 30 min. The chromogen was developed with 3,3′-diaminobenzidine (DAB; Dako). All steps were separated by Tris buffer (Dako) washes and performed at room temperature. All histological stains were performed by histology cores at Indiana University (IU) School of Medicine.

PanIN Analysis in KC Mice

Using a standard H&E slide, small clusters of abnormal ducts were looked at as a first target. Using the Johns Hopkins School of Medicine classification system,[88] clusters of abnormal ducts were classified into PanIN grades 0 (normal), 1-A, 1-B, 2, and 3. Each duct in the cluster was scored, and PanIN size analysis was done using the Aperio Imagescope system.

Fibrosis and Immune Response Quantification

Slides were analyzed using Aperio Imagescope and the Food and Drug Administration (FDA)-approved algorithm with few a modifications. The entire pancreatic tissue was analyzed, with the exclusion of vessels, lymph nodes, and peri-pancreatic fat.

Trichrome

An FDA-approved algorithm was altered to detect blue against a red background. Hue value was altered from 0.1 (brown) to 0.62 (blue), hue width was altered from 0.5 to 0.4, and color saturation was altered from 0.04 to 0.005.

Sirius Red

Hue value was altered from 0.1 (brown) to 0.85 (red), and hue width was not changed. Color saturation was altered from 0.04 to 0.6. The intensity threshold was lowered from 175 to 100.

B220

A pathologist reviewed the slides and determined the quantity of cells that were B220-positive.

Immunostaining

Serial frozen sections (5–7 μm) were rehydrated in PBS, permeabilized with 0.5% Triton X solution, blocked with 10% BSA, and probed with either αSMA antibody (Novus Biologicals, NB500-631, 1:200), CK19 antibody (Abcam, ab52625, 1:200), insulin antibody (Cell Signaling Technology, 4590S, 1:200), or α-Amylase (Cell Signaling Technology, 3796S, 1:200) overnight at 4°C. Epitope retrieval was performed using 1× sodium citrate buffer, followed by Triton X permeabilization. Subsequently, slides were stained with the secondary antibody Alexa Fluor 594 goat anti-rabbit IgG (Life Technologies, A11037, 1:1,000). Slides were mounted with Vectashield antifade mounting medium with DAPI (Vector Laboratories, H-1200), and coverslips were sealed.

GFP Immunohistochemistry

Paraffin-embedded tissues were sectioned (5 μm), and epitope retrieval was performed using heat-induced epitope retrieval (HIER) with 10 mM citrate buffer. Endogenous peroxidase activity was blocked using 3% H_2O_2 in methanol and subsequently blocked with 0.5% BSA. Primary antibody, mouse anti-GFP (Cell Signaling Technology, 2955, 1:200), was applied and incubated overnight at 4°C. Secondary anti-mouse IgG was utilized from the Vectastain mouse IgG ABC kit (Vector Labs, PK-6102) and developed with peroxidase substrate solution consisting of 0.05% DAB and 0.01% H_2O_2 in PBS according to the manufacturer's protocol. Sections were counterstained in Gill no. 1 hematoxylin (Leica Biosystems, 3801520), cleared, and mounted with a resin-based mounting medium.

Retrograde Pancreatic Ductal Delivery

Mice were sedated using isoflurane with 1.5%–3% oxygen, the abdominal cavity was opened, and a customized catheter was inserted into the cystic duct through a small opening at the bottom of the gallbladder. The catheter was then advanced into the common bile duct and secured in place with a microclamp around the bile duct and catheter to prevent vector reflux into the liver. A microclamp was placed on the sphincter of Oddi to avoid leakage of the vector into the duodenum, and 100 μL of AAV vector containing the GFP transgene or PBS (vehicle control) was slowly infused into the pancreatic duct through the catheter. Successful administration was documented by uniform swelling of the gland. The microclamps used to temporarily block liver infusion and duodenum leakage were released 5 min after the infusion was completed. The catheter was then removed, the inner abdominal cavity was closed with absorbable sutures, and the outer skin was closed with wound clips. Post-surgery, mice were placed on a heating pad to maintain body temperature during recovery. After the animals recovered, they were returned to their cages. Mice were treated subcutaneously with carprofen (5–10 mg/kg) to prevent post-operative discomfort.

Mice

KC mice were generated as described previously.[12] Conditional *LSL-Kras^{G12D}* mice were crossed with *Pdx1-Cre* animals to generate the KC mice. All animal housing, use, and surgical procedures were carried out in accordance with the regulatory guidelines set by Guide for the Care and Use of Laboratory Animals of the NIH. All animal protocols were reviewed and approved by the IU and The Research Institute at Nationwide Children's Hospital Animal Care and Use Committees.

Statistical Analysis

Student's t test and ANOVA with Tukey post hoc analysis were used for statistical analysis. Data are presented as mean, and error bars represent SEM.

SUPPLEMENTAL INFORMATION

Supplemental Information includes two figures and three tables and can be found with this article online at https://doi.org/10.1016/j.omtm.2017.09.006.

AUTHOR CONTRIBUTIONS

K.A.Q. and J.J.K. generated all figures. K.A.Q. prepared sections. J.J.K. performed immunofluorescence staining and imaging and assisted J.K. with dosing, necropsy, and tissue collection in normal mice. A.A. performed GFP transduction quantification in AAV6-, AAV8-, and AAV9-dosed mice. T.F. and K.A.Q. performed quantification of GFP expression in various pancreatic cell types. C.J.T. performed Sirius Red staining. M.J. and G.E.S. performed quantification of Sirius Red staining, B220 marker, and PanIN grade/size analysis. K.S. assisted J.K. with dosing of PDAC mice, necropsy, and tissue collection. L.G.C. helped J.K. optimize the intraductal delivery technique using Evans Blue dye and assisted with preparing customized catheters. K.R.C. and J.T.M. guided the experimental design. K.R.C. and M.K. edited the manuscript, and M.K. imaged representative PanIN lesions. J.K. conceived the project, developed the experimental plan, performed intraductal infusions, monitored the study/data collection, and wrote the manuscript.

ACKNOWLEDGMENTS

This work was supported in part by grants from the IU Simon Cancer Center, CTSI NIH/NCRR Project Development Team (UL1TR001108), the Showalter Trust Foundation, and an American Cancer Society institutional research grant (to J.K.) and the NCI (CA-075059) (to M.K.). J.J.K. was supported by the Cagiantas Scholarship and NCI Grant 1 F31 CA213731-01A1. The authors would also like to thank Jerry R. Mendell (The Research Institute at Nationwide Children's Hospital, Columbus, Ohio), who provided advice and discussions of this manuscript.

REFERENCES

1. Dimastromatteo, J., Brentnall, T., and Kelly, K.A. (2017). Imaging in pancreatic disease. Nat. Rev. Gastroenterol. Hepatol. *14*, 97–109.
2. Eliasson, M., Talbäck, M., and Rosén, M. (2008). Improved survival in both men and women with diabetes between 1980 and 2004–a cohort study in Sweden. Cardiovasc. Diabetol. *7*, 32.
3. Xiao, A.Y., Tan, M.L., Wu, L.M., Asrani, V.M., Windsor, J.A., Yadav, D., and Petrov, M.S. (2016). Global incidence and mortality of pancreatic diseases: a systematic review, meta-analysis, and meta-regression of population-based cohort studies. Lancet Gastroenterol. Hepatol. *1*, 45–55.
4. Rahib, L., Smith, B.D., Aizenberg, R., Rosenzweig, A.B., Fleshman, J.M., and Matrisian, L.M. (2014). Projecting cancer incidence and deaths to 2030: the unexpected burden of thyroid, liver, and pancreas cancers in the United States. Cancer Res. *74*, 2913–2921.
5. Von Hoff, D.D., Ervin, T., Arena, F.P., Chiorean, E.G., Infante, J., Moore, M., Seay, T., Tjulandin, S.A., Ma, W.W., Saleh, M.N., et al. (2013). Increased survival in pancreatic cancer with nab-paclitaxel plus gemcitabine. N. Engl. J. Med. *369*, 1691–1703.
6. Conroy, T., Desseigne, F., Ychou, M., Bouché, O., Guimbaud, R., Bécouarn, Y., Adenis, A., Raoul, J.L., Gourgou-Bourgade, S., de la Fouchardière, C., et al.; Groupe Tumeurs Digestives of Unicancer; PRODIGE Intergroup (2011). FOLFIRINOX versus gemcitabine for metastatic pancreatic cancer. N. Engl. J. Med. *364*, 1817–1825.
7. Siegel, R.L., Miller, K.D., and Jemal, A. (2017). Cancer Statistics, 2017. CA Cancer J. Clin. *67*, 7–30.
8. Ryan, D.P., Hong, T.S., and Bardeesy, N. (2014). Pancreatic adenocarcinoma. N. Engl. J. Med. *371*, 2140–2141.
9. Mazur, P.K., and Siveke, J.T. (2012). Genetically engineered mouse models of pancreatic cancer: unravelling tumour biology and progressing translational oncology. Gut *61*, 1488–1500.
10. Morris, J.P., 4th, Wang, S.C., and Hebrok, M. (2010). KRAS, Hedgehog, Wnt and the twisted developmental biology of pancreatic ductal adenocarcinoma. Nat. Rev. Cancer *10*, 683–695.
11. Hingorani, S.R., Wang, L., Multani, A.S., Combs, C., Deramaudt, T.B., Hruban, R.H., Rustgi, A.K., Chang, S., and Tuveson, D.A. (2005). Trp53R172H and KrasG12D cooperate to promote chromosomal instability and widely metastatic pancreatic ductal adenocarcinoma in mice. Cancer Cell *7*, 469–483.
12. Hingorani, S.R., Petricoin, E.F., Maitra, A., Rajapakse, V., King, C., Jacobetz, M.A., Ross, S., Conrads, T.P., Veenstra, T.D., Hitt, B.A., et al. (2003). Preinvasive and invasive ductal pancreatic cancer and its early detection in the mouse. Cancer Cell *4*, 437–450.
13. Grippo, P.J., and Tuveson, D.A. (2010). Deploying mouse models of pancreatic cancer for chemoprevention studies. Cancer Prev. Res. (Phila.) *3*, 1382–1387.
14. Carrière, C., Gore, A.J., Norris, A.M., Gunn, J.R., Young, A.L., Longnecker, D.S., and Korc, M. (2011). Deletion of Rb accelerates pancreatic carcinogenesis by oncogenic Kras and impairs senescence in premalignant lesions. Gastroenterology *141*, 1091–1101.
15. Biankin, A.V., Waddell, N., Kassahn, K.S., Gingras, M.C., Muthuswamy, L.B., Johns, A.L., Miller, D.K., Wilson, P.J., Patch, A.M., Wu, J., et al.; Australian Pancreatic Cancer Genome Initiative (2012). Pancreatic cancer genomes reveal aberrations in axon guidance pathway genes. Nature *491*, 399–405.
16. Waddell, N., Pajic, M., Patch, A.M., Chang, D.K., Kassahn, K.S., Bailey, P., Johns, A.L., Miller, D., Nones, K., Quek, K., et al.; Australian Pancreatic Cancer Genome Initiative (2015). Whole genomes redefine the mutational landscape of pancreatic cancer. Nature *518*, 495–501.
17. Ying, H., Dey, P., Yao, W., Kimmelman, A.C., Draetta, G.F., Maitra, A., and DePinho, R.A. (2016). Genetics and biology of pancreatic ductal adenocarcinoma. Genes Dev. *30*, 355–385.
18. Li, X., Wu, R., and Ventura, A. (2016). The present and future of genome editing in cancer research. Hum. Genet. *135*, 1083–1092.
19. Tschaharganeh, D.F., Lowe, S.W., Garippa, R.J., and Livshits, G. (2016). Using CRISPR/Cas to study gene function and model disease in vivo. FEBS J. *283*, 3194–3203.
20. Chira, S., Gulei, D., Hajitou, A., Zimta, A.A., Cordelier, P., and Berindan-Neagoe, I. (2017). CRISPR/Cas9: Transcending the Reality of Genome Editing. Mol. Ther. Nucleic Acids *7*, 211–222.
21. Chiou, S.H., Winters, I.P., Wang, J., Naranjo, S., Dudgeon, C., Tamburini, F.B., Brady, J.J., Yang, D., Grüner, B.M., Chuang, C.H., et al. (2015). Pancreatic cancer modeling using retrograde viral vector delivery and in vivo CRISPR/Cas9-mediated somatic genome editing. Genes Dev. *29*, 1576–1585.
22. Yu, X., Zhang, Y., Chen, C., Yao, Q., and Li, M. (2010). Targeted drug delivery in pancreatic cancer. Biochim. Biophys. Acta *1805*, 97–104.
23. Ramamoorth, M., and Narvekar, A. (2015). Non viral vectors in gene therapy- an overview. J. Clin. Diagn. Res. *9*, GE01–GE06.
24. Al-Dosari, M.S., and Gao, X. (2009). Nonviral gene delivery: principle, limitations, and recent progress. AAPS J. *11*, 671–681.
25. Doiron, B., Hu, W., Norton, L., and DeFronzo, R.A. (2012). Lentivirus shRNA Grb10 targeting the pancreas induces apoptosis and improved glucose tolerance due to decreased plasma glucagon levels. Diabetologia *55*, 719–728.

26. Montini, E., Cesana, D., Schmidt, M., Sanvito, F., Bartholomae, C.C., Ranzani, M., Benedicenti, F., Sergi, L.S., Ambrosi, A., Ponzoni, M., et al. (2009). The genotoxic potential of retroviral vectors is strongly modulated by vector design and integration site selection in a mouse model of HSC gene therapy. J. Clin. Invest. *119*, 964–975.

27. Heckl, D., Schwarzer, A., Haemmerle, R., Steinemann, D., Rudolph, C., Skawran, B., Knoess, S., Krause, J., Li, Z., Schlegelberger, B., et al. (2012). Lentiviral vector induced insertional haploinsufficiency of Ebf1 causes murine leukemia. Mol. Ther. *20*, 1187–1195.

28. Raper, S.E., and DeMatteo, R.P. (1996). Adenovirus-mediated in vivo gene transfer and expression in normal rat pancreas. Pancreas *12*, 401–410.

29. Ayuso, E., Chillón, M., Agudo, J., Haurigot, V., Bosch, A., Carretero, A., Otaegui, P.J., and Bosch, F. (2004). In vivo gene transfer to pancreatic beta cells by systemic delivery of adenoviral vectors. Hum. Gene Ther. *15*, 805–812.

30. Wang, A.Y., Peng, P.D., Ehrhardt, A., Storm, T.A., and Kay, M.A. (2004). Comparison of adenoviral and adeno-associated viral vectors for pancreatic gene delivery in vivo. Hum. Gene Ther. *15*, 405–413.

31. Sigalla, J., David, A., Anegon, I., Fiche, M., Huvelin, J.M., Boeffard, F., Cassard, A., Soulillou, J.P., and Le Mauff, B. (1997). Adenovirus-mediated gene transfer into isolated mouse adult pancreatic islets: normal beta-cell function despite induction of an anti-adenovirus immune response. Hum. Gene Ther. *8*, 1625–1634.

32. McClane, S.J., Chirmule, N., Burke, C.V., and Raper, S.E. (1997). Characterization of the immune response after local delivery of recombinant adenovirus in murine pancreas and successful strategies for readministration. Hum. Gene Ther. *8*, 2207–2216.

33. Wang, Z., Zhu, T., Rehman, K.K., Bertera, S., Zhang, J., Chen, C., Papworth, G., Watkins, S., Trucco, M., Robbins, P.D., et al. (2006). Widespread and stable pancreatic gene transfer by adeno-associated virus vectors via different routes. Diabetes *55*, 875–884.

34. Xiao, X., Guo, P., Prasadan, K., Shiota, C., Peirish, L., Fischbach, S., Song, Z., Gaffar, I., Wiersch, J., El-Gohary, Y., et al. (2014). Pancreatic cell tracing, lineage tagging and targeted genetic manipulations in multiple cell types using pancreatic ductal infusion of adeno-associated viral vectors and/or cell-tagging dyes. Nat. Protoc. *9*, 2719–2724.

35. Cheng, H., Wolfe, S.H., Valencia, V., Qian, K., Shen, L., Phillips, M.I., Chang, L.J., and Zhang, Y.C. (2007). Efficient and persistent transduction of exocrine and endocrine pancreas by adeno-associated virus type 8. J. Biomed. Sci. *14*, 585–594.

36. Guo, P., Xiao, X., El-Gohary, Y., Criscimanna, A., Prasadan, K., Rymer, C., Shiota, C., Wiersch, J., Gaffar, I., Esni, F., and Gittes, G.K. (2013). Specific transduction and labeling of pancreatic ducts by targeted recombinant viral infusion into mouse pancreatic ducts. Lab. Invest. *93*, 1241–1253.

37. Xiao, X., Gaffar, I., Guo, P., Wiersch, J., Fischbach, S., Peirish, L., Song, Z., El-Gohary, Y., Prasadan, K., Shiota, C., and Gittes, G.K. (2014). M2 macrophages promote beta-cell proliferation by up-regulation of SMAD7. Proc. Natl. Acad. Sci. USA *111*, E1211–E1220.

38. Xiao, X., Prasadan, K., Guo, P., El-Gohary, Y., Fischbach, S., Wiersch, J., Gaffar, I., Shiota, C., and Gittes, G.K. (2014). Pancreatic duct cells as a source of VEGF in mice. Diabetologia *57*, 991–1000.

39. Chen, M., Maeng, K., Nawab, A., Francois, R.A., Bray, J.K., Reinhard, M.K., Boye, S.L., Hauswirth, W.W., Kaye, F.J., Aslanidi, G., et al. (2017). Efficient Gene Delivery and Expression in Pancreas and Pancreatic Tumors by Capsid-Optimized AAV8 Vectors. Hum. Gene Ther. Methods *28*, 49–59.

40. Loiler, S.A., Tang, Q., Clarke, T., Campbell-Thompson, M.L., Chiodo, V., Hauswirth, W., Cruz, P., Perret-Gentil, M., Atkinson, M.A., Ramiya, V.K., and Flotte, T.R. (2005). Localized gene expression following administration of adeno-associated viral vectors via pancreatic ducts. Mol. Ther. *12*, 519–527.

41. Kota, J., Handy, C.R., Haidet, A.M., Montgomery, C.L., Eagle, A., Rodino-Klapac, L.R., Tucker, D., Shilling, C.J., Therlfall, W.R., Walker, C.M., et al. (2009). Follistatin gene delivery enhances muscle growth and strength in nonhuman primates. Sci. Transl. Med. *1*, 6ra15.

42. Bennett, J., Wellman, J., Marshall, K.A., McCague, S., Ashtari, M., DiStefano-Pappas, J., Elci, O.U., Chung, D.C., Sun, J., Wright, J.F., et al. (2016). Safety and durability of effect of contralateral-eye administration of AAV2 gene therapy in patients with childhood-onset blindness caused by RPE65 mutations: a follow-on phase 1 trial. Lancet *388*, 661–672.

43. Hastie, E., and Samulski, R.J. (2015). Adeno-associated virus at 50: a golden anniversary of discovery, research, and gene therapy success–a personal perspective. Hum. Gene Ther. *26*, 257–265.

44. McCarty, D.M., Monahan, P.E., and Samulski, R.J. (2001). Self-complementary recombinant adeno-associated virus (scAAV) vectors promote efficient transduction independently of DNA synthesis. Gene Ther. *8*, 1248–1254.

45. McCarty, D.M., Fu, H., Monahan, P.E., Toulson, C.E., Naik, P., and Samulski, R.J. (2003). Adeno-associated virus terminal repeat (TR) mutant generates self-complementary vectors to overcome the rate-limiting step to transduction in vivo. Gene Ther. *10*, 2112–2118.

46. McCarty, D.M. (2008). Self-complementary AAV vectors; advances and applications. Mol. Ther. *16*, 1648–1656.

47. McClane, S.J., Hamilton, T.E., Burke, C.V., and Raper, S.E. (1997). Functional consequences of adenovirus-mediated murine pancreatic gene transfer. Hum. Gene Ther. *8*, 739–746.

48. Rehman, K.K., Trucco, M., Wang, Z., Xiao, X., and Robbins, P.D. (2008). AAV8-mediated gene transfer of interleukin-4 to endogenous beta-cells prevents the onset of diabetes in NOD mice. Mol. Ther. *16*, 1409–1416.

49. Shimony, N., Bendayan, M., Elkin, G., Ben-nun-Shaul, O., Abd-El-Latif, M., Scherzer, P., Arbel, O., Ziv, E., Krasny, L., Pizov, G., et al. (2008). Pancreatic acinar and islet cell infection by low-dose SV40 administration. Pancreas *36*, 411–416.

50. Phillips, N., and Kay, M.A. (2014). Characterization of vector-based delivery of neurogenin-3 in murine diabetes. Hum. Gene Ther. *25*, 651–661.

51. Griffin, M.A., Restrepo, M.S., Abu-El-Haija, M., Wallen, T., Buchanan, E., Rokhlina, T., Chen, Y.H., McCray, P.B., Jr., Davidson, B.L., Divekar, A., and Uc, A. (2014). A novel gene delivery method transduces porcine pancreatic duct epithelial cells. Gene Ther. *21*, 123–130.

52. Nakai, H., Fuess, S., Storm, T.A., Muramatsu, S., Nara, Y., and Kay, M.A. (2005). Unrestricted hepatocyte transduction with adeno-associated virus serotype 8 vectors in mice. J. Virol. *79*, 214–224.

53. Inagaki, K., Fuess, S., Storm, T.A., Gibson, G.A., Mctiernan, C.F., Kay, M.A., and Nakai, H. (2006). Robust systemic transduction with AAV9 vectors in mice: efficient global cardiac gene transfer superior to that of AAV8. Mol. Ther. *14*, 45–53.

54. GuhaSarkar, D., Su, Q., Gao, G., and Sena-Esteves, M. (2016). Systemic AAV9-IFNβ gene delivery treats highly invasive glioblastoma. Neuro-oncol. *18*, 1508–1518.

55. Mendell, J.R., Sahenk, Z., Malik, V., Gomez, A.M., Flanigan, K.M., Lowes, L.P., Alfano, L.N., Berry, K., Meadows, E., Lewis, S., et al. (2015). A phase 1/2a follistatin gene therapy trial for Becker muscular dystrophy. Mol. Ther. *23*, 192–201.

56. Mendell, J.R., Rodino-Klapac, L.R., Rosales, X.Q., Coley, B.D., Galloway, G., Lewis, S., Malik, V., Shilling, C., Byrne, B.J., Conlon, T., et al. (2010). Sustained alpha-sarcoglycan gene expression after gene transfer in limb-girdle muscular dystrophy, type 2D. Ann. Neurol. *68*, 629–638.

57. Jimenez, V., Ayuso, E., Mallol, C., Agudo, J., Casellas, A., Obach, M., Muñoz, S., Salavert, A., and Bosch, F. (2011). In vivo genetic engineering of murine pancreatic beta cells mediated by single-stranded adeno-associated viral vectors of serotypes 6, 8 and 9. Diabetologia *54*, 1075–1086.

58. Sato, T., Miyashita, E., Yamauchi, H., and Matsuno, S. (1986). The role of surgical treatment for chronic pancreatitis. Ann. Surg. *203*, 266–271.

59. Sherman, S., and Lehman, G.A. (1991). ERCP- and endoscopic sphincterotomy-induced pancreatitis. Pancreas *6*, 350–367.

60. Laukkarinen, J.M., Van Acker, G.J., Weiss, E.R., Steer, M.L., and Perides, G. (2007). A mouse model of acute biliary pancreatitis induced by retrograde pancreatic duct infusion of Na-taurocholate. Gut *56*, 1590–1598.

61. Wildi, S., Kleeff, J., Mayerle, J., Zimmermann, A., Böttinger, E.P., Wakefield, L., Büchler, M.W., Friess, H., and Korc, M. (2007). Suppression of transforming growth factor beta signalling aborts caerulein induced pancreatitis and eliminates restricted stimulation at high caerulein concentrations. Gut *56*, 685–692.

62. Testoni, P.A., Bagnolo, F., Caporuscio, S., and Lella, F. (1999). Serum amylase measured four hours after endoscopic sphincterotomy is a reliable predictor of post-procedure pancreatitis. Am. J. Gastroenterol. *94*, 1235–1241.

63. Braganza, J.M., Lee, S.H., McCloy, R.F., and McMahon, M.J. (2011). Chronic pancreatitis. Lancet *377*, 1184–1197.

64. Kwon, J.J., Nabinger, S.C., Vega, Z., Sahu, S.S., Alluri, R.K., Abdul-Sater, Z., Yu, Z., Gore, J., Nalepa, G., Saxena, R., et al. (2015). Pathophysiological role of microRNA-29 in pancreatic cancer stroma. Sci. Rep. *5*, 11450.

65. Kota, J., Hancock, J., Kwon, J., and Korc, M. (2017). Pancreatic cancer: Stroma and its current and emerging targeted therapies. Cancer Lett. *391*, 38–49.

66. Hyman, D.M., Taylor, B.S., and Baselga, J. (2017). Implementing Genome-Driven Oncology. Cell *168*, 584–599.

67. Kannan, R., and Ventura, A. (2015). The CRISPR revolution and its impact on cancer research. Swiss Med. Wkly. *145*, w14230.

68. Dow, L.E. (2015). Modeling Disease In Vivo With CRISPR/Cas9. Trends Mol. Med. *21*, 609–621.

69. Kato, T., and Takada, S. (2017). In vivo and in vitro disease modeling with CRISPR/Cas9. Brief. Funct. Genomics *16*, 13–24.

70. Han, Y.C., Vidigal, J.A., Mu, P., Yao, E., Singh, I., González, A.J., Concepcion, C.P., Bonetti, C., Ogrodowski, P., Carver, B., et al. (2015). An allelic series of miR-17 ~ 92-mutant mice uncovers functional specialization and cooperation among members of a microRNA polycistron. Nat. Genet. *47*, 766–775.

71. Concepcion, C.P., Bonetti, C., and Ventura, A. (2012). The microRNA-17-92 family of microRNA clusters in development and disease. Cancer J. *18*, 262–267.

72. van Rooij, E., Sutherland, L.B., Thatcher, J.E., DiMaio, J.M., Naseem, R.H., Marshall, W.S., Hill, J.A., and Olson, E.N. (2008). Dysregulation of microRNAs after myocardial infarction reveals a role of miR-29 in cardiac fibrosis. Proc. Natl. Acad. Sci. USA *105*, 13027–13032.

73. Xie, J., Ameres, S.L., Friedline, R., Hung, J.H., Zhang, Y., Xie, Q., Zhong, L., Su, Q., He, R., Li, M., et al. (2012). Long-term, efficient inhibition of microRNA function in mice using rAAV vectors. Nat. Methods *9*, 403–409.

74. He, X., Xie, J., Zhang, D., Su, Q., Sai, X., Bai, R., Chen, C., Luo, X., Gao, G., and Pan, W. (2015). Recombinant adeno-associated virus-mediated inhibition of microRNA-21 protects mice against the lethal schistosome infection by repressing both IL-13 and transforming growth factor beta 1 pathways. Hepatology *61*, 2008–2017.

75. Sicard, F., Gayral, M., Lulka, H., Buscail, L., and Cordelier, P. (2013). Targeting miR-21 for the therapy of pancreatic cancer. Mol. Ther. *21*, 986–994.

76. van Rooij, E., and Kauppinen, S. (2014). Development of microRNA therapeutics is coming of age. EMBO Mol. Med. *6*, 851–864.

77. Knabel, M.K., Ramachandran, K., Karhadkar, S., Hwang, H.W., Creamer, T.J., Chivukula, R.R., Sheikh, F., Clark, K.R., Torbenson, M., Montgomery, R.A., et al. (2015). Systemic Delivery of scAAV8-Encoded MiR-29a Ameliorates Hepatic Fibrosis in Carbon Tetrachloride-Treated Mice. PLoS ONE *10*, e0124411.

78. Kota, J., Chivukula, R.R., O'Donnell, K.A., Wentzel, E.A., Montgomery, C.L., Hwang, H.W., Chang, T.C., Vivekanandan, P., Torbenson, M., Clark, K.R., et al. (2009). Therapeutic microRNA delivery suppresses tumorigenesis in a murine liver cancer model. Cell *137*, 1005–1017.

79. Hsu, S.H., Wang, B., Kota, J., Yu, J., Costinean, S., Kutay, H., Yu, L., Bai, S., La Perle, K., Chivukula, R.R., et al. (2012). Essential metabolic, anti-inflammatory, and anti-tumorigenic functions of miR-122 in liver. J. Clin. Invest. *122*, 2871–2883.

80. Ma, H.I., Hueng, D.Y., Shui, H.A., Han, J.M., Wang, C.H., Lai, Y.H., Cheng, S.Y., Xiao, X., Chen, M.T., and Yang, Y.P. (2014). Intratumoral decorin gene delivery by AAV vector inhibits brain glioblastomas and prolongs survival of animals by inducing cell differentiation. Int. J. Mol. Sci. *15*, 4393–4414.

81. Wu, Q.J., Gong, C.Y., Luo, S.T., Zhang, D.M., Zhang, S., Shi, H.S., Lu, L., Yan, H.X., He, S.S., Li, D.D., et al. (2012). AAV-mediated human PEDF inhibits tumor growth and metastasis in murine colorectal peritoneal carcinomatosis model. BMC Cancer *12*, 129.

82. Crommentuijn, M.H., Kantar, R., Noske, D.P., Vandertop, W.P., Badr, C.E., Würdinger, T., Maguire, C.A., and Tannous, B.A. (2016). Systemically administered AAV9-sTRAIL combats invasive glioblastoma in a patient-derived orthotopic xenograft model. Mol. Ther. Oncolytics *3*, 16017.

83. Streck, C.J., Dickson, P.V., Ng, C.Y., Zhou, J., Hall, M.M., Gray, J.T., Nathwani, A.C., and Davidoff, A.M. (2006). Antitumor efficacy of AAV-mediated systemic delivery of interferon-beta. Cancer Gene Ther. *13*, 99–106.

84. Wang, B., Li, J., and Xiao, X. (2000). Adeno-associated virus vector carrying human minidystrophin genes effectively ameliorates muscular dystrophy in mdx mouse model. Proc. Natl. Acad. Sci. USA *97*, 13714–13719.

85. Haidet, A.M., Rizo, L., Handy, C., Umapathi, P., Eagle, A., Shilling, C., Boue, D., Martin, P.T., Sahenk, Z., Mendell, J.R., and Kaspar, B.K. (2008). Long-term enhancement of skeletal muscle mass and strength by single gene administration of myostatin inhibitors. Proc. Natl. Acad. Sci. USA *105*, 4318–4322.

86. Rodino-Klapac, L.R., Janssen, P.M., Shontz, K.M., Canan, B., Montgomery, C.L., Griffin, D., Heller, K., Schmelzer, L., Handy, C., Clark, K.R., et al. (2013). Micro-dystrophin and follistatin co-delivery restores muscle function in aged DMD model. Hum. Mol. Genet. *22*, 4929–4937.

87. Clark, K.R., Liu, X., McGrath, J.P., and Johnson, P.R. (1999). Highly purified recombinant adeno-associated virus vectors are biologically active and free of detectable helper and wild-type viruses. Hum. Gene Ther. *10*, 1031–1039.

88. Hruban, R.H., Adsay, N.V., Albores-Saavedra, J., Compton, C., Garrett, E.S., Goodman, S.N., Kern, S.E., Klimstra, D.S., Klöppel, G., Longnecker, D.S., et al. (2001). Pancreatic intraepithelial neoplasia: a new nomenclature and classification system for pancreatic duct lesions. Am. J. Surg. Pathol. *25*, 579–586.